Experimental Mechanics (2019) 59:319–325
https://doi.org/10.1007/s11340-018-00444-5

Faster Sickling Kinetics and Sickle Cell Shape Evolution during Repeated Deoxygenation and Oxygenation Cycles

E. Du[1,2] · M. Dao[1]

Received: 31 May 2018 / Accepted: 22 October 2018 / Published online: 28 November 2018

Abstract

Kinetics of cell sickling and morphological change have been recognized as important parameters that are correlated closely with altered blood rheology and vasoocclusion in microcirculation. A microfluidic transient hypoxia assay was developed to create repeated hypoxia-normoxia cycles for real time observation of repetitive sickling and unsickling of freely suspended red blood cells (RBCs) from sickle cell disease patients. Cell sickling behavior and kinetics were found to be influenced by its previous sickling-unsickling processes accumulatively, where those sickled RBCs that had a history of sickling in a previous hypoxia cycle would sickle again in subsequent hypoxia/sickling cycles and the collective sickling kinetics became progressively faster (with reduced delay time and higher sickled fraction versus deoxygenation time). Individual sickled RBCs would sickle into drastically different shapes randomly in subsequent hypoxia/sickling cycles, however, the collective shape distribution retained similar characteristics. These observations indicate a gradual worsening trend in sickling kinetics over repeated hypoxia cycles, as well as a relatively stable collective shape characteristics within a limited number of hypoxia-normoxia cycles.

Keywords Microfluidics · Sickle cell disease · HbS polymerization · Cell morphology · Cyclic hypoxia-normoxia

Introduction

Intracellular polymerization of deoxygenated sickle hemoglobin (HbS) causes poorly deformable, distorted red blood cells (RBCs) in sickle cell disease (SCD) [1]. This process is known as cell sickling and is a key pathophysiologic event in SCD. HbS polymerization is associated with cell dehydration and increased cell density (higher HbS concentration), which further accelerate the process of HbS polymerization and cell sickling [2].

The repetitive deoxygenation-oxygenation (DeOxy-Oxy) cycles exerted on sickle RBCs in blood circulation induce cyclic polymerization-depolymerization of HbS and consequently cyclic cell sickling-unsickling. These repeated processes cause accumulated damages to sickle cells, result in cell dehydration, poor deformability, hemolysis, and are associated with deleterious effects on the vasculature [3] and impaired blood flow [4]. The additional shear stresses exerted on sickle RBCs from blood flow in branched and size-varying vasculatures may pose severe cyclic mechanical loading to cell membrane and accelerate the damage process of sickle RBCs. Early *in vitro* studies on morphology of sickle RBCs undergoing continuing cell sickling-unsickling processes showed different observations. In the study by Padilla et al. [5], sickle RBCs were challenged by 100% O_2 and 100% N_2 and exhibited no identical cell deformations. In the study by Coletta et al. [6], cell sickling was triggered by photodissociation of CO bonded-hemoglobin and exhibited a "memory" effect in cell transformation of its previous cycle(s). Therefore, a platform with controlled hypoxia to mimic repeated DeOxy-Oxy cycles in blood flow is needed and will provide a basis for the study of intracellular HbS polymerization-depolymerization and associated cell sickling-unsickling as well as altered blood rheology in SCD.

Microfluidics provides an ideal platform to control the oxygen microenvironment for the study of single sickle cells [7, 8]. In this paper, we report an *in vitro* study of repetitive sickling and unsickling of sickle RBCs that are freely suspended in RPMI-1640 culture medium. Morphological change in RBCs exposed to transient hypoxia-normoxia cycles in the microfluidic assay showed a direct correlation between the cell morphology and the

Electronic supplementary material The online version of this article (https://doi.org/10.1007/s11340-018-00444-5) contains supplementary material, which is available to authorized users.

✉ M. Dao
mingdao@mit.edu

[1] Department of Materials Science and Engineering, Massachusetts Institute of Technology, Cambridge, MA 02139, USA

[2] Department of Ocean and Mechanical Engineering, Florida Atlantic University, Boca Raton, FL 33431, USA

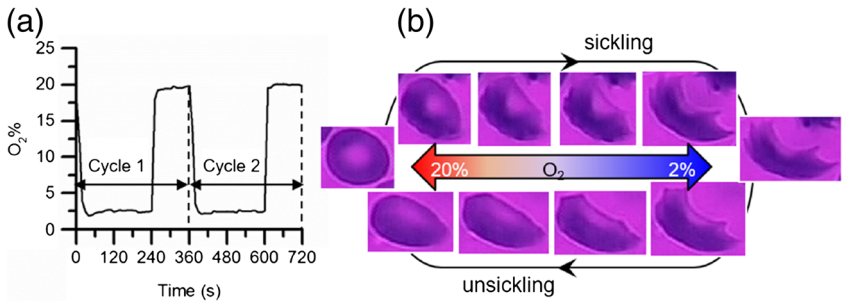

Fig. 1 *In vitro* transient hypoxia-induced cell sickling and unsickling. (A) Repeated DeOxy-Oxy cycles. (B) Sickling and unsickling of a representative sickle RBC during one cycle of imposed transient hypoxia

level of oxygen in the cell suspension (Fig. 1). A time lapse of cell shape evolution in response to the transient hypoxia indicates that the *in vitro* hypoxia-induced cell sickling starts with initiation of intracellular HbS polymerization, mostly away from the dimple area, follows by growth of HbS polymers, and eventually protrudes and severely distorts cell membrane, e.g. from a biconcave, disc shape to a typical sickled shape. This observation suggests that nucleation of the HbS polymers may start near the inner surface of the membrane away from the dimple area. A reoxygenation (ReOxy) induced-cell unsickling exhibits an opposite process to the cell sickling process. The HbS fibers that protrude/distort cell membrane melt first, followed by further dissolution of the polymerized HbS inside the cell membrane, and eventually the whole cell goes back to its original biconcave shape. While shear flow, cell-cell interactions, and DeOxy rate are likely to be additional contributors to influence cell sickling process and their morphological evolution *in vivo*, here in this study we focus on the inherent cell sickling kinetics and shape changes due to repeated DeOxy-Oxy cycles. We demonstrate that repeated cell sickling-unsickling process can be captured in such microfluidic environment with physiologically relevant gas conditions and DeOxy-Oxy cycles. This setup quantifies the parameters associated with cell shape evolution due to HbS polymerization (DeOxy) and depolymerization (Oxy) in individually tracked cells. Repeated sickling/unsickling cycles on longer time scales or scenarios of complex Oxy-DeOxy cycles that are closer to the *in vivo* circulation conditions may lead to more interesting cellular responses, which can be implemented by modifying the current experimental setup in future investigations.

Materials and Methods

RBC Preparation

Blood samples were collected under an Excess Human Material Protocol approved by the Partners Healthcare Institutional Review Board with a waiver of consent. Blood samples from 6 patients with homozygous SCD and undergoing hydroxyurea therapy were studied. Samples were collected in EDTA anticoagulant at the Massachusetts General Hospital and delivered to the Massachusetts Institute of Technology on ice and stored at 4 °C before measurement. The sample pool has an HbS level varying from 66.9% to 90.4% and a Fetal hemoglobin level varying from 6.3% to 29.8%. A volume of 1 ml of each blood sample was washed twice with Phosphate Buffered Saline at 2000 rpm for 5 min at 21 °C. A volume of 5 μl RBCs was carefully pipetted from the pellet and fully suspended by gentle vortexing in 1 ml RPMI-1640 containing 1% *w/v* Bovine Serum Albumin (Sigma-Aldrich, St Louis, MO).

Cyclic Hypoxia Assay

Transient hypoxia environment was created using a microfluidics technique described in our previous publication [7]. In summary, the microfluidic hypoxia assay consisted of a double-layer structure, fabricated using standard polydimethylsiloxane (PDMS) casting protocols and bonded to a microscope cover slip via air plasma. Temperature within the microfluidic assay was maintained at 37 °C using a heating incubator (Ibidi heating system). Sickle RBC suspension was loaded in the cell channel, which was separated by a thin PDMS membrane from the gas channel. O_2 concentration in the freely suspended RBCs was then controlled by the gas mixture in the gas channel: fully oxygenated state was created by an oxygen-rich gas mixture (5% CO_2, 20% O_2, and 75% N_2) and deoxygenated state was created by an oxygen-poor gas mixture (5% CO_2, 2% O_2, and 93% N_2). A transient hypoxia-normoxia cycle was created by switching between these two gas supplies at fixed time intervals (Fig. 1). During each cycle, the oxygen-poor gas mixture was supplied to the gas channel and maintained for 4 min, then the oxygen-rich gas mixture was supplied and maintained for 2 min, resulting in a 220-s hypoxia ($O_2 < 5\%$) and a 140-s Oxy state (O_2 concentration > 5%). This design allowed real time monitoring of morphological change in individual RBCs during repeated continuing DeOxy-Oxy cycles on a Zeiss Axiovert 200 inverted microscope (Carl Zeiss Inc., Thornwood, NY).

RBC Sickling Analysis

Microscopic video of sickle cells subjected to repeated DeOxy-Oxy cycles was recorded at 1 frame per second. Cell

sickling was identified by morphologic changes of sickle RBCs. The image of cells was visually enhanced with a 414/46 nm bandpass filter (Semrock), which matches the optical absorption spectra for Oxy-hemoglobin and DeOxy-hemoglobin [9]. Sickling analysis was carried out in two aspects, including morphology and kinetics of cell sickling. To quantify the morphological change with cell sickling process subjected to repeated DeOxy-Oxy cycles, circular shape factor (CSF) and elliptical shape factor (ESF) [10] are calculated from $CSF = 4\pi A/P^2$ and $ESF = D_a/D_b$, where A represents the projected area of the cell, P represents its perimeter, D_a and D_b represents the short and long axis of the best-fit ellipse of the cell. Values of the required parameters for each sickle RBC were determined using ImageJ [11].

Kinetics of cell sickling was quantified by sickled fraction, delay time of cell sickling and completion time for cell sickling. Sickled fraction was calculated as the percentage of cells undergoing morphological sickling over all RBCs. Delay time of cell sickling is defined as the time elapsed between the initiation of DeOxy and the point when a cell shows visually identifiable features of morphological sickling, i.e. changes in cell shape, texture, and darkness (see the Methods in [7] for more details). Completion time for cell sickling is defined as the duration for a sickle RBC to complete the sickling process, starting from the emergence of any optically visible changes to the point when the same cell exhibits a fully sickled shape (i.e. no further morphological changes can be observed) during the DeOxy process. In this study, only those cells showing morphological changes were counted for the delay time and completion time for cell sickling.

Statistical analyses were performed with OriginPro 9 (OriginLab Corporation, Northampton, MA). All data were expressed as mean ± SD, unless stated otherwise. A two-sample t test between measurements of samples during different cycles was used to generate the p values. A p value of less than 0.05 was considered statistically significant.

Results

Changes in Cell Morphology

The *in vitro* hypoxia assay provided a real-time monitoring of individual sickle RBCs (See Video S1 in the supplementary material). Tracking individual cells for their morphological changes during the repeated DeOxy-Oxy cycles demonstrated a lack of "memory" in the shape of the same individual sickled cells under current hypoxic conditions (Fig. 2). There seems to be no obvious correlation between consecutive DeOxy cycles that a sickled cell goes back to a specific shape. Cell morphological sickling initiated randomly at cell edges based on the individually tracked cells in the stationary suspension (Fig. 2A). Five representative sickle RBCs with minor structural markers (such as spicules or defects on cell membrane) were selected to demonstrate this finding. A blue arrow was used to indicate the reference orientation of the projected image of a selected cell. Yellow arrow(s) was used to mark the initial sites where the cell membranes started to deform by the intracellular HbS polymer strands or clusters (dark regions as shown in the figures). This process can be identified from the microscopic video recording by tracking individual cells as the absorption peak of DeOxy-HbS shifts from that of Oxy-HbS, making cells containing DeOxy-HbS appear significantly darker than those containing Oxy-HbS. Additionally, along with the polymerization of DeOxy-HbS, dense clusters of HbS fibers make cells appear even darker than those containing less HbS aggregates. Changes in the cell membranes may initiate from single site or multiple sites. During each of the DeOxy processes, the fully sickled RBCs displayed very different shapes (Fig. 2B). Five representative cells, including three discocytes and two irreversibly sickled cells were selected to demonstrate the difference in shapes during the five-consequent DeOxy processes. This was observed in majority of cells in the present study. Interestingly, those severely deformed RBCs were able to fully recover to their individual original relaxed shapes during a subsequent ReOxy process, without apparent membrane loss (vesiculation) or any visually obvious permanent damage. This demonstrates a lack of significant "plastic deformation" in cell membranes for freely suspended cells challenged by a limited number of hypoxia-normoxia cycles.

Shape factors ESF and CSF were used to characterize quantitatively the degree of deviation of a sickle RBC from a circular shape and the degree of elongation, respectively. A perfect discocyte has $ESF = CSF = 1$. Majority of Oxy-sickle RBCs has values of ESF and CSF close to 1 (Fig. 3A). During the initial Oxy state, a large fraction of sickle RBCs were discocytes based on 377 sickle RBCs randomly picked and analyzed from 6 patient samples. There was about 57% of cells with CSF value greater than 0.88 and ESF value greater than 0.80. Mean values of CSF and ESF were 0.87 ± 0.07 and 0.80 ± 0.13 for Oxy 1 and 0.87 ± 0.06 and 0.81 ± 012 for Oxy 6. The slight shift in the histograms of CSF-ESF distributions after 5 DeOxy-Oxy cycles was not statistically significant. On the other hand, hypoxia-induced HbS polymerization distorted cell membranes drastically as indicated by the wide distributions of ESF and CSF (Fig. 3B). Mean values of CSF and ESF were 0.63 ± 0.11 and 0.65 ± 0.15 for DeOxy 1and 0.65 ± 0.11 and 0.67 ± 0.14 for DeOxy 5. Interestingly, although individual sickled RBCs showed drastically different shapes during different DeOxy processes, collectively, there was no significant changes in cell shapes as showed by the similar distributions of ESF-CSF values for sickled RBCs during DeOxy 1 and DeOxy 5 (Fig. 3B). These observations indicate a potential retention of sickle RBCs to keep their characteristic shapes collectively within a limited number of hypoxia-normoxia cycles.

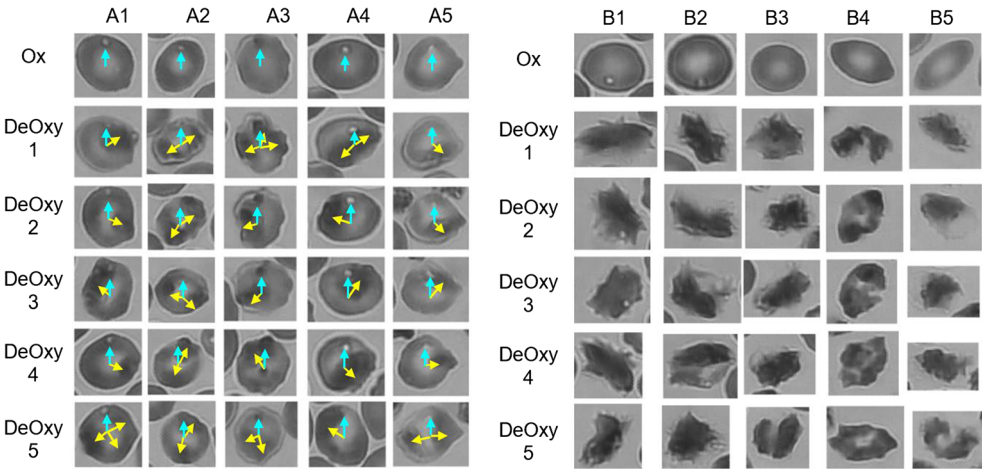

Fig. 2 Randomness in hypoxia-induced cellular morphological sickling during repeated DeOxy-Oxy cycles. (A) Initiation site(s) of membrane deformation indicates the primary site(s) for growth of intracellular HbS polymers, highlighted with yellow arrows, with respect to the vertical orientation of individually tracked sickle RBCs highlighted with blue arrows. (B) Heterogeneity in shapes of fully sickled RBCs for discocytes (B1 - B3) and irreversibly sickled cells (B4 & B5)

Kinetics of Cell Sickling

We observed a large variation in sickled fraction values among different patient samples. During the first DeOxy cycle, the sample with the lowest HbS level (67%) and highest HbF level (29.8%) had a lowest sickled fraction value of 12%, while the one with the highest HbS level (90.4%) and lowest HbF level (6%) had a highest sickled fraction value of 81%. Sickled fraction and delay time of cell sickling were determined to examine the effects of repeated DeOxy-Oxy cycles on individual sickle RBCs. Values of sickled fraction for a representative sample increased gradually from 55% to 57%, 59%, 61% and 62% through the five DeOxy-Oxy cycles (Fig. 4A). This is due to the emergence of new sickled RBCs during each additional DeOxy process while those cells that sickled in a previous cycle continued to sickle. The delay time of cell sickling decreased with the DeOxy cycle number. This indicates a slightly increased whole cell sickling rate from a faster polymerization process of DeOxy-HbS, likely due to the undissolved HbS polymers from a previous cycle. Delay time of cell sickling for 60 sickle RBCs in a representative sample decreased from 69 ± 28 s to 63 ± 32 s, 62 ± 34 s, 60 ± 30 s, and 59 ± 34 s through the 5 DeOxy-Oxy cycles (Fig. 4B). Both parameters indicate that previous sickling-unsickling processes can affect the cell sickling during a subsequent DeOxy-Oxy cycle.

This trend in sickled fraction was found throughout the 6 patient samples in the present study but with a significant variation (Fig. 5A) between different patients. To compare between samples, each parameter was normalized to the value determined from the first DeOxy process for the specific patient sample. Interestingly, although the patient sample with the highest HbF level (also with the lowest HbS level, open circles in red color) has the lowest absolute sickled fraction, the normalized sickled fraction increased rapidly along with the DeOxy-Oxy cycles. Those samples with relatively higher HbS levels (asterisk and diamond symbols) had relatively smaller increase in the normalized sickled fraction as not many additional cells become sickled during the subsequent DeOxy-Oxy cycles. Delay time of cell sickling decreased

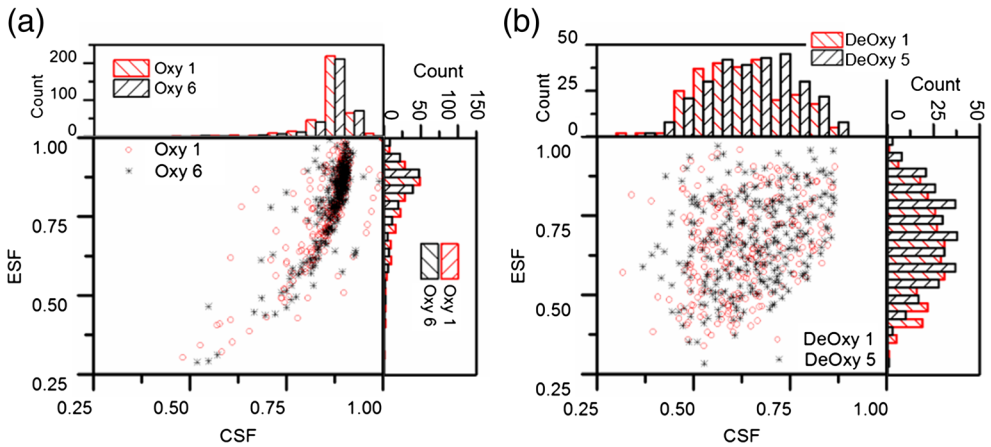

Fig. 3 Morphological changes in sickle RBCs during DeOxy-Oxy cycles: (A) ESF-CSF scatter graph of cells during the initial Oxy process (red open symbols, $n = 377$) and during the ReOxy process (black asterisks, $n = 351$) after five repeated DeOxy-Oxy cycles; (B) ESF-CSF scatter plots of cells during the initial DeOxy (red open symbols, $n = 254$) and during the fifth DeOxy process (black asterisks, $n = 290$). Each symbol corresponds to 1 sickle cell. Corresponding histograms represent the distribution of the ESF and CSF values

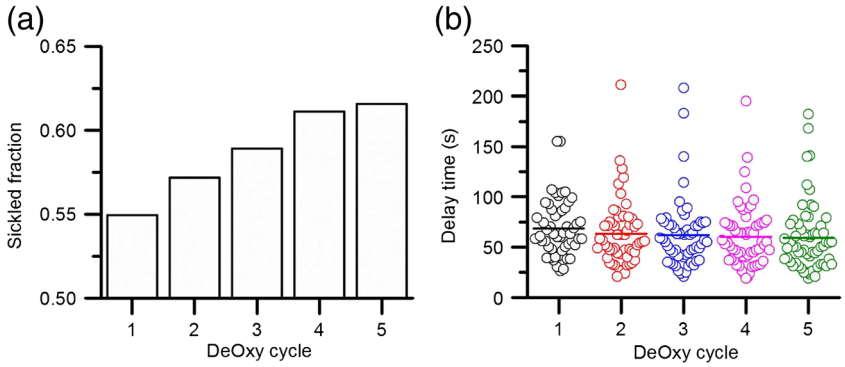

Fig. 4 Kinetics of cell sickling for a representative sample: (A) sickled fraction and (B) delay time of cell sickling during the cyclic DeOxy-Oxy processes. Horizontal lines in the scatter plot show the mean values based on 60 cells

consistently with the DeOxy-Oxy cycles (Fig. 5B), which was observed throughout the 6 samples in the present study, irrespective of the HbS and HbF levels.

Tracking of 134 cells randomly picked from different patient samples showed that the completion of cell sickling process takes place in as short as less than l second to more than 15 s (Fig. 6). This range is consistent with the observations in a previous study of cell sickling where cells were exposed to 100% N_2 [5]. Average value of the delay time decreased significantly ($p < 0.001$) from 78.6 ± 39.7 s for DeOxy 1 to 52.0 ± 35.4 s for DeOxy 5, which is the primary factor that causes the shift in the scatter graph of completion time and delay time. Average value of the completion time increased from 5.3 ± 2.3 s for DeOxy 1 to 6.2 ± 3.0 s for DeOxy 5 ($p < 0.01$). The increase in the overall time for the completion of cell sickling are contributed by those newly emerged sickled RBCs during additional DeOxy-Oxy cycles, which likely contain less HbS and require more time to polymerize.

Discussion and Concluding Remarks

It is known that cell sickling requires intracellular fiber formation through extensive polymer alignment [6]. This can lead to a delay in cell sickling, which is considered important to prevent most sickle RBCs from sickling during *in vivo* circulation [12]. In the present study, the average delay time of all 6 patient samples ranged from 109 ± 30 s during the initial DeOxy and decreased to 81 s ± 14 s during the fifth DeOxy cycle. This process is diffusion-based (similar to the DeOxy process *in vivo*), which is much slower than the polymerization process of HbS in solution and in cells induced by pohotolysis of intracellular carboxy hemoglobin with an argon ion laser focused inside the cell [13]. This delay time in cell sickling plus the time required for a cell to complete its sickling process (in a range from less than 1 s to more than 15 s) could provide the needed time for many or even majority of sickle cells to escape from the narrowest vasculatures *in vivo* with low O_2 before turning into rigid, sickled cells that are more likely to clog these smallest openings in microcirculation. However, the hypoxia-induced cell sickling events can be influenced by its previous sickling-unsickling processes. Those sickled RBCs that had a history of sickling in a previous cycle retained their "memory" and would sickle again in subsequent hypoxia-normoxia cycles. Changes in the kinetics of cell sickling during the repeated DeOxy-Oxy cycles, including the gradually decreased cell sickling delay time and the increased sickled fraction due to newly emerged sickled cells during each additional DeOxy process, may lead to more and more sickle RBCs that sickle faster under the same hypoxic conditions and increase the chance of vasoocclusion after going through repeated DeOxy-Oxy cycles *in vivo*.

Observed membrane deformation based on individually tracked sickle RBCs showed that the shape change induced by DeOxy-HbS polymers often started away from the dimple area and differed from cycle to cycle. It should be noted that

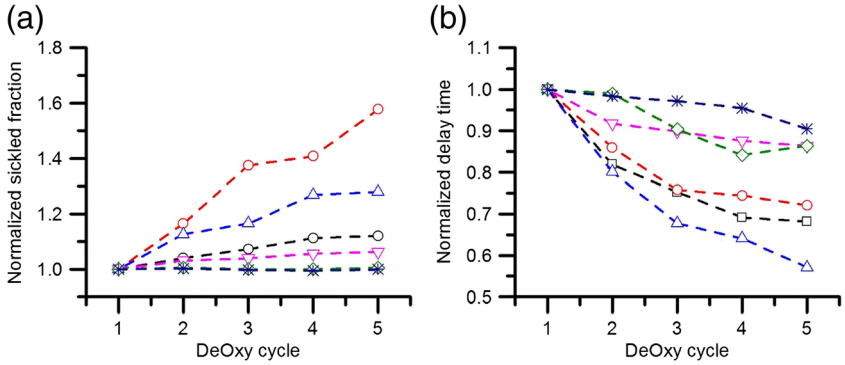

Fig. 5 Kinetics of cell sickling among different samples in response to DeOxy-Oxy cycling: (A) normalized sickled fraction and (B) normalized delay time of cell sickling. Open symbols represent the normalized values determined during each DeOxy-Oxy cycle; each dashed line represents an individual patient sample

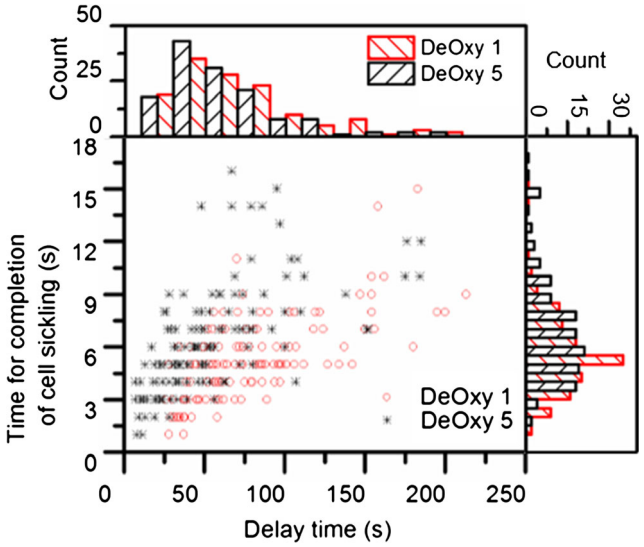

Fig. 6 Scatter graph of time for completion of cell sickling and delay time of cell sickling for individual sickle RBCs during cycle number DeOxy 1 and DeOxy 5. Each point represents 1 of 134 cells

those initiation sites were not always associated with the visual defects of cell membrane. This observation indicated that formation of the primary HbS fibers may be enhanced at those particular sites on the cell membrane, which may also point to possible leaking sites with higher K efflux and Na influx [14]. This observation also partially agrees with a previous study demonstrating HbS retains a "memory" of previous sickling cycles [6]. The same study also showed the cell always deformed along the same axis during subsequent cycles. This is discrepant from our observations and another study [5] where the same cell did not present the identical deformation at the fully sickled state during cyclic hypoxia. This discrepancy may be due to the difference in the DeOxy rate between the photochemically induced cell sickling and diffusion-driven hypoxia induced cell sickling. Deformation of individual sickle cells was found to be random during repetitive hypoxia, which may be due to the randomly branched HbS polymers after the primary polymerization at the particular sites at cell edges. This can be explained by a 2-step mechanism of HbS polymerization [15] and agrees with the observations of "unpredictable polymerization of HbS" under extreme DeOxy (100% N_2) conditions [5].

Morphology analysis indicated a lack of "apparent plastic deformation" in cell membrane during limited repetitive hypoxia cycles for individually tracked sickle RBCs. The evidence is that the fully sickled RBCs always recovered to their initial relaxed state with cell membrane visually intact after each cycle of ReOxy. Collectively, values of ESF and CSF of sickled RBCs indicated a certain retention in keeping the cell shapes. This reluctance in cell shape change may help maintain a relatively steady blood rheology *in vivo* as the blood viscosity is highly dependent on the shapes of sickled RBCs, confirmed by a recent computational simulation study [8]. We note that RBCs may significantly change shape due to vesiculation [16]. A prior study [17] showed sickle cells lose their lipid as spectrin-free hemoglobin-containing spicules, which are likely due to the imposed long-term hypoxia condition (1-h N_2 incubation) and/or the additional centrifugation forces that contributed to the shedding of the spicules from the cell membranes. Another study [18] showed the generation of spectrin-free membrane vesicles by mechanical force generated from micropipette aspiration. The membrane vesiculation for sickle RBCs may occur under a harsh condition, through gradually formation in the normal aging process or during repeated sickling *in vivo*. However, in the present study with only a limited number of DeOxy-Oxy cycles (5 cycles in 30 min as compared to ~10^4 cycles in a typical 15-day lifespan of sickle cells *in vivo*), no signs of membrane vesiculation or membrane shedding were observed directly. Another possible factor is the "free suspension" condition in our *in vitro* assay, which is less severe than the *in vivo* circulation condition where cells are subjected to more complicated flow dynamics and cell-cell interactions in the vasculatures. These conditions can be considered in future studies.

In summary, our microfluidic platform provides a single-cell based robust quantitative measurement of cell sickling/unsickling in response to the repeated DeOxy-Oxy cycles mimicking the oxygen exchange during *in vivo* circulation. Cell sickling behavior and kinetics were apparently influenced by the previous sickling-unsickling cycles in an accumulative manner, where those previously sickled RBCs in a previous hypoxia cycle would retain their "memory" and sickle again in subsequent hypoxia/sickling cycles; and the collective sickling kinetics would become progressively faster with reduced delay time and higher sickled fraction versus more deoxygenation cycles. These observations indicate a gradual worsening trend in sickling kinetics over repeated hypoxia cycles. With respect to cell shape evolution, individual sickled RBCs would sickle into drastically different shapes randomly in subsequent hypoxia/sickling cycles, however, the collective shape distribution retained similar characteristics. The collective reluctance in cell shape change and no noticeable permanent damages in cell membranes within a limited number of repeated DeOxy-Oxy cycles, may help maintain a relatively "steady state" in blood rheology over certain period of time.

Acknowledgements The work was supported by National Institutes of Health (NIH) Grants U01HL114476 and R01HL121386. E.D. acknowledges support by the National Science Foundation (NSF) under Grant No. 1635312 and Florida Atlantic University faculty startup grant. The authors thank Dr. John Higgins for providing sickle blood samples and for helpful discussions and Dr. Monica Diez-Silva for help with sample preparation and insightful discussions.

References

1. Eaton WA, Hofrichter J (1987) Hemoglobin-S Gelation and Sickle-Cell Disease. Blood 70(5):1245–1266

2. Brugnara C (1995) Erythrocyte dehydration in pathophysiology and treatment of sickle cell disease. Curr Opin Hematol 2(2):132–138
3. Zhou Z, Yee DL, Guchhait P (2012) Molecular Link between Intravascular Hemolysis and Vascular Occlusion in Sickle Cell Disease. Curr Vasc Pharmacol 10(6):756–761
4. Ballas SK, Mohandas N (2004) Sickle red cell microrheology and sickle blood rheology. Microcirculation 11(2):209–225
5. Padilla F, Bromberg PA, Jensen WN (1973) The sickle-unsickle cycle: a cause of cell fragmentation leading to permanently deformed cells. Blood 41(5):653–660
6. Coletta M, Alayash AI, Wilson MT, Benedetti PA, Evangelista V, Brunori M (1988) Single Cell Microspectroscopy Reveals That Erythrocytes Containing Hemoglobin-S Retain a Memory of Previous Sickling Cycles. FEBS Lett 236(1):127–131
7. Du E, Diez-Silva M, Kato GJ, Dao M, Suresh S (2015) Kinetics of sickle cell biorheology and implications for painful vasoocclusive crisis. Proc Natl Acad Sci U S A 112(5):1422–1427
8. Li X, Du E, Lei H, Tang Y-H, Dao M, Suresh S, Karniadakis GE (2016) Patient-specific blood rheology in sickle-cell anaemia. Interface Focus 6(1):20150065
9. Zhujun Z, Seitz WR (1986) Optical Sensor for Oxygen Based on Immobilized Hemoglobin. Anal Chem 58(1):220–222
10. Asakura T, Asakura K, Obata K, Mattiello J, Ballas SK (2005) Blood samples collected under venous oxygen pressure from patients with sickle cell disease contain a significant number of a new type of reversibly sickled cells: Constancy of the percentage of sickled cells in individual patients during steady state. Am J Hematol 80(4):249–256
11. Rasband WS, ImageJ U, Health NIo. Bethesda, Maryland, USA, 1997–2011. Image J
12. Mozzarelli A, Hofrichter J, Eaton WA (1987) Delay Time of Hemoglobin-S Polymerization Prevents Most Cells from Sickling Invivo. Science 237(4814):500–506
13. Coletta M, Hofrichter J, Ferrone FA, Eaton WA (1982) Kinetics of Sickle Hemoglobin Polymerization in Single Red-Cells. Nature 300(5888):194–197
14. Hebbel RP (1991) Beyond Hemoglobin Polymerization - the Red-Blood-Cell Membrane and Sickle Disease Pathophysiology. Blood 77(2):214–237
15. Galkin O, Vekilov PG (2004) Mechanisms of homogeneous nucleation of polymers of sickle cell anemia hemoglobin in deoxy state. J Mol Biol 336(1):43–59
16. Li H, Lu L, Li X, Buffet PA, Dao M, Karniadakis GE, Suresh S (2018) Mechanics of diseased red blood cells in human spleen and consequences for hereditary blood disorders. Proc Natl Acad Sci U S A 115(38):9574–9579
17. Allan D, Limbrick AR, Thomas P, Westerman MP (1982) Release of spectrin-free spicules on reoxygenation of sickled erythrocytes. Nature 295(5850):612–613
18. Knowles DW, Tilley L, Mohandas N, Chasis JA (1997) Erythrocyte membrane vesiculation: model for the molecular mechanism of protein sorting. Proc Natl Acad Sci U S A 94(24):12969–12974